

Diffusion-Driven Domain Adaptation for Generating 3D Molecules

Haokai Hong¹ Wanyu Lin¹ Kay Chen Tan¹

Abstract

Can we train a molecule generator that can generate 3D molecules from a new domain, circumventing the need to collect data? This problem can be cast as the problem of domain adaptive molecule generation. This work presents a novel and principled diffusion-based approach, called *GADM*, that allows shifting a generative model to desired new domains without the need to collect even a single molecule. As the domain shift is typically caused by the structure variations of molecules, e.g., scaffold variations, we leverage a designated equivariant masked autoencoder (MAE) along with various masking strategies to capture the structural-grained representations of the in-domain varieties. In particular, with an asymmetric encoder-decoder module, the MAE can generalize to unseen structure variations from the target domains. These structure variations are encoded with an equivariant encoder and treated as domain supervisors to control denoising. We show that, with these encoded structural-grained domain supervisors, *GADM* can generate effective molecules within the desired new domains. We conduct extensive experiments across various domain adaptation tasks over benchmarking datasets. We show that our approach can improve up to 65.6% in terms of success rate defined based on molecular validity, uniqueness, and novelty compared to alternative baselines.

1. Introduction

Geometric generative models are proposed to approximate the distribution of complex geometries and are used to generate feature-rich geometries. They have emerged as a crucial research direction in various scientific fields (e.g., material science, biology, and chemistry (Hoogeboom et al., 2022; Watson et al., 2023; Xie et al., 2022)), attempting to facili-

¹Department of Computing, The Hong Kong Polytechnic University. Correspondence to: Wanyu Lin <wanyu.lin@polyu.edu.hk>.

Under Review. Preprint.

Table 1. Alternative baselines were trained with QM9, a canonical molecule dataset. Source, target I, and target II domains encompass molecules with high-, low-, and rare-frequency scaffolds, respectively. The generated samples from EDM and GeoLDM, which are trained on molecules with source scaffolds, are dominated by the training scaffold set, indicating that they can well reflect the training data distribution.

	QM9 Scaffold Proportion (%)		
	Source Domain	Target Domain I	Target Domain II
QM9	76.4	11.5	12.1
EDM	90.9	5.9	2.7
GeoLDM	90.6	5.9	3.5

tate the process of scientific knowledge discovery. In these fields, geometries could be point clouds where each point is embedded in the Cartesian coordinates and encompasses rich features. For example, 3D molecules can be represented as atomic geometric graphs (Hoogeboom et al., 2022; Xu et al., 2023; Song et al., 2024b).

There has been fruitful research progress on 3D molecule generation based on geometric generative modeling due to their ability to estimate density and generate feature-rich geometries. Recent representative models for generating 3D molecules in silicon include autoregressive (Luo & Ji, 2022), flow-based models (Garcia Satorras et al., 2021), and diffusion models (Hoogeboom et al., 2022). Among others, diffusion models have demonstrated their superior performance in terms of various empirical evaluation metrics, such as stability and validity (Hoogeboom et al., 2022). However, these generative models are trained to mimic the training data distribution, limiting their capability within the in-domain generation and manipulation (Han et al., 2024), *i.e.*, controllable generation.

With the expressive power of the state-of-the-art diffusion-based generators, *can we train a diffusion-based molecule generator that can flexibly adapt to a desired new domain where data are scarce and difficult to collect?* This problem can be cast as a domain adaptive generation problem, whose goal is to shift the data distribution of generators to a desired new domain different from what it is trained over. In the context of molecule generation, the distribution shift mainly comes from structure variations (Wu et al., 2018; Lee et al., 2023). The structure variation could be the various types of scaffolds or ring-structures.

Taking a canonical molecule dataset – QM9 as our running example, diverse scaffolds of molecules have varying proportions in nature (Ramakrishnan et al., 2014; Wu et al., 2018). We observed that EDM (Hooeboom et al., 2022) and GeoLDM (Xu et al., 2023) indeed could capture the training data distribution well — generating molecules with scaffolds existing in the high-frequency class — but they struggle to generate molecules with low-frequency scaffolds (see Table 1). Our preliminary study proves the excellent expressive capability of the current diffusion-based molecule generators. On the other hand, it indicates the difficulty in generating molecules deviating from the training data distribution. Existing works for domain adaptive generation are tailed for specific generation tasks, such as image (Song et al., 2024a), dialog (Qian & Yu, 2019), and question-answering generation (Yang et al., 2017). As far as we know, ours is the first work to consider domain adaptive generation for 3D molecules.

To address the above issues, we develop a new and principled diffusion-based generator, called **Geometric Adaptive Diffusion Model (GADM)**, that can adaptively synthesize 3D molecules in the desired new domains. In particular, **GADM** enables the generation of 3D molecules with structural-grained variations adaptively, including the distribution shifts due to scaffold and ring-structure variations, respectively. The underlying assumption is that if we can capture the set of structure variations right, generalizing the unseen ones that ultimately lead to the target domain is a much easier process. Using QM9 as an example (see Table 1, source, target I, and target II are three domains due to scaffold variations. Our proposed generator **GADM** is trained with source molecules — the high-frequency scaffolds. Once trained, **GADM** can generate molecules with low/rare-frequency scaffolds conditioned on corresponding scaffolds in target I/target II.

The crux of **GADM** is to empower the denoising process with domain priors, which is characterized by a designated **Equivariant Masked Autoencoder (EMAE)**. Our **EMAE** is realized with an asymmetric encoder-decoder architecture, enabling to capture the domain priors — in-domain structure variations and to generalize to out-of-domain structure variations (He et al., 2022). More specifically, during training, the in-domain priors, such as scaffolds or ring-structures from the source domain, are encoded and subsequently act as domain supervisors to control the denoising process of **Domain Supervised Diffusion Model (DSDM)**. In the generation phase, the generalization capability provided by the asymmetric **EMAE** allows for properly encoding the unseen structure variations, i.e., scaffolds or rings from the target domains. These captured target domain priors are used to control the denoising process to generate 3D molecules within the desired new domains.

To ensure that the generated 3D molecules are $SE(3)$ -equivariant, our **EMAE** employs the well-known equivariant graph neural network module to encode the structural-grained domain supervisors. Notably, unlike prior domain adaption works (Song et al., 2024a), **GADM** does not need additional training for the entire adaptive generation process. In a nutshell, our main contributions are delineated as follows.

First, we pioneer the domain adaptive generation problem in the context of 3D molecule generation. Correspondingly, we propose a geometric adaptive diffusion-based generation framework capable of adaptively generating target molecules outside the training domain without additional training. In particular, we adopt the idea of **Masked Autoencoder (MAE)** to extract latent features of in-domain and out-of-domain supervisors for conditional denoising in diffusion models. *Second*, we proved that the domain supervisor extracted by the designed **EMAE** is $SE(3)$ -equivariant, ensuring the molecular generation is equivariant. *Third*, to validate the effectiveness of the proposed framework, we compare it with EDM (Hooeboom et al., 2022) and GeoLDM (Xu et al., 2023) over benchmarking datasets. Extensive experimental results demonstrate that the latent features, acting as domain supervisors, empower the diffusion models to generate molecules with desired structural variations adaptively. Remarkably, the success rate of generated molecules by **GADM** is improved by up to 65.6% compared with existing methods. Our work represents a significant advancement in generating novel molecules that are absent in the training samples but exhibit the desired structural variations.

2. Problem Setup and Preliminaries

2.1. Problem Definition

Notations: Let d be the dimensionality of node features; a 3D molecule can be represented as a point cloud denoted as $\mathcal{G} = \langle \mathbf{x}, \mathbf{h} \rangle$, where $\mathbf{x} = (\mathbf{x}_1, \dots, \mathbf{x}_N) \in \mathbb{R}^{N \times 3}$ is the atom coordinate matrix and $\mathbf{h} = (\mathbf{h}_1, \dots, \mathbf{h}_N) \in \mathbb{R}^{N \times d}$ is the node feature matrix containing atomic type, charge features, etc. For a given molecule \mathcal{G} , the scaffold is its structural framework (Bemis & Murcko, 1996), termed as “chemotypes,” which could be regarded as a subgraph of the original molecule, represented as $\mathcal{G}^s = \langle \mathbf{x}^s, \mathbf{h}^s \rangle$. Except for scaffolds, the ring structures are essential in Chemistry and Biology (Karageorgis et al., 2014; Ward & Beswick, 2014; Ritchie & Macdonald, 2009), which could also be a factor that incurs the distribution shift.

Domain Adaptive Generation Problem: We consider the problem of domain adaptive generation in the following two scenarios, including scaffold-domain and ring-structure-domain adaptive generation, respectively.

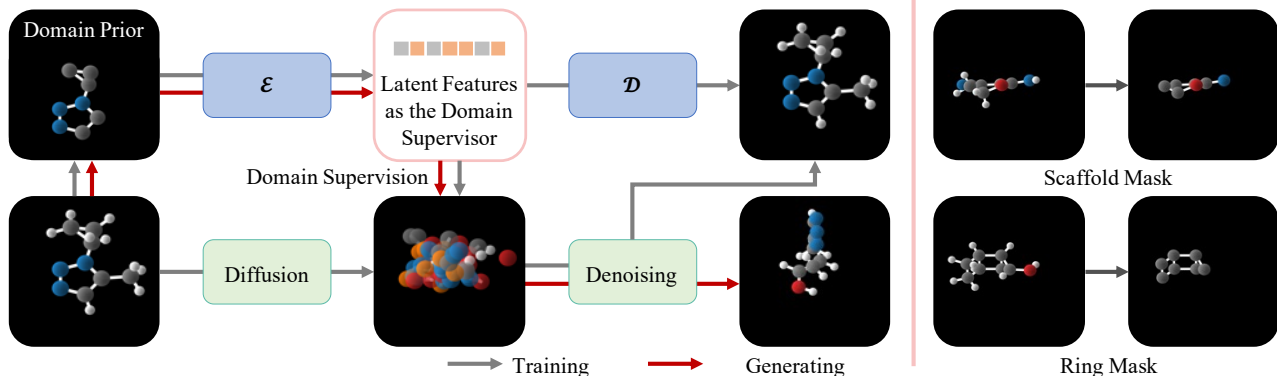


Figure 1. The Illustration of Proposed GADM Framework.

During training (gray pipeline): I. Equivariant Masked Autoencoder (EMAE): the equivariant encoder (\mathcal{E}) first maps the domain prior—masked structure (i.e. scaffold/ring)—into the masked latent features. These latent features would be processed with an equivariant decoder (\mathcal{D}) for reconstructing the original molecule in 3D atomic space. This asymmetric encoder-decoder architecture enables to capture the in-domain priors and to generalize to out-of-domain structures. II. Domain Prior-Supervised Diffusion Model (DSDM): DSDM first diffuses the molecule into noises and then incorporates the masked latent features as domain supervisor to perform denoising for reconstructing the input molecules.

During generation (red pipeline): EMAE receives the target domain prior and encodes it as the domain supervisor. Then, DSDM denoises from sampled Gaussian noise under domain supervision to generate novel and valid molecules with target structure variations.

Given a collection of molecules as training samples and corresponding scaffold/ring-structure set denoted as $\{\mathcal{G}_S\}$, $\{\mathcal{G}_S^s\}$, respectively. For simplicity, we call the training sample domain as the source domain. Domain adaptive generation aims to learn a generative model that can generate valid and novel molecules falling into a targeted new domain, where corresponding scaffold/ring-structure set is $\{\mathcal{G}_T^s\}$, and the targeted scaffold/ring-structure set is unseen during training, a.k.a. $\{\mathcal{G}_S^s\} \cap \{\mathcal{G}_T^s\} = \emptyset$.

2.2. Preliminaries

Equivariance. Molecules, typically existing within a three-dimensional physical space, are subject to geometric symmetries, including translations, rotations, and potential reflections. These are collectively referred to as the Euclidean group in 3 dimensions, denoted as $E(3)$ (Celeghini et al., 1991).

A function F is said to be equivariant to the action of a group G if $T_g \circ F(\mathbf{x}) = F \circ S_g(\mathbf{x})$ for all $g \in G$, where S_g, T_g are linear representations related to the group element g (Serre et al., 1977). For geometric graph generation, we consider the special Euclidean group $SE(3)$, involving translations and rotations. Moreover, the transformations S_g or T_g can be represented by a translation \mathbf{t} and an orthogonal matrix rotation \mathbf{R} . For a molecule $\mathcal{G} = \langle \mathbf{x}, \mathbf{h} \rangle$, the node features \mathbf{h} are $SE(3)$ -invariant while the coordinates \mathbf{x} are $SE(3)$ -equivariant, which can be expressed as $\mathbf{R}\mathbf{x} + \mathbf{t} = (\mathbf{R}\mathbf{x}_1 + \mathbf{t}, \dots, \mathbf{R}\mathbf{x}_N + \mathbf{t})$.

Diffusion Models. Diffusion models (Sohl-Dickstein et al., 2015) are latent variable models for learning distributions by modeling the reverse of a diffusion process (Ho et al.,

2020). Given a data point $\mathbf{x}_0 \sim q(\mathbf{x}_0)$ and a variance schedule β_1, \dots, β_T that controls the amount of noise added at each timestep t , the diffusion process or forward process gradually add Gaussian noise to the data point \mathbf{x} :

$$q(\mathbf{x}_t | \mathbf{x}_{t-1}) := \mathcal{N}(\mathbf{x}_t; \sqrt{1 - \beta_t} \mathbf{x}_{t-1}, \beta_t \mathbf{I}), \quad (1)$$

Generally, the diffusion process q has no trainable parameters. The denoising process or reverse process aims at learning a parameterized generative process, which incrementally denoise the noisy variables $\mathbf{x}_{T:1}$ to approximately restore the data point \mathbf{x}_0 in the original data distribution:

$$p_\theta(\mathbf{x}_{t-1} | \mathbf{x}_t) := \mathcal{N}(\mathbf{x}_{t-1}; \mu_\theta(\mathbf{x}_t, t), \Sigma_\theta(\mathbf{x}_t, t)), \quad (2)$$

where the initial distribution $p(\mathbf{x}_t)$ is sampled from standard Gaussian noise $\mathcal{N}(0, \mathbf{I})$. The loss for training diffusion model $\mathcal{L}_{DM} := \mathcal{L}_t$ is simplified as:

$$\mathcal{L}_{DM} = \mathbb{E}_{\mathbf{x}_0, \epsilon, t} [w(t) \|\epsilon - \epsilon_\theta(\mathbf{x}_t, t)\|^2], \quad (3)$$

where $w(t) = \frac{\beta_t}{2\sigma_t^2 \alpha_t (1 - \bar{\alpha}_t)}$ is the reweighting term and could be simply set as 1 with promising sampling quality, and $\mathbf{x}_t = \sqrt{\bar{\alpha}_t} \mathbf{x}_0 + \sqrt{1 - \bar{\alpha}_t} \epsilon$. We provide detailed description about diffusion models in Appendix.

3. Method

Overview. Our objective is to learn a generator with the source domain with rich data that can flexibly adapt to a new domain in a low-data regime. Generally, structure variations, such as scaffold or ring-structure variations, are the main cause of the domain shift in the context of molecule generation (Wu et al., 2018; Lee et al., 2023). We particularly

focus on the geometric adaptive generation problem where the scaffold/ring-structure set of the source domain, represented as $\{\mathcal{G}_S^s\}$, and the targeted scaffold/ring-structure set from new domains, denoted as $\{\mathcal{G}_T^s\}$, are different. In other words, the targeted scaffold/ring-structure set of the target domain is unseen during training — $\{\mathcal{G}_S^s\} \cap \{\mathcal{G}_T^s\} = \emptyset$.

With the superior capability of diffusion models for 3D molecule generation, we propose to address the geometric domain adaptive molecule generation problem with a diffusion engine. However, as illustrated in Section 1, the vanilla diffusion models have difficulty generating out-of-domain molecules. In this regard, we propose to incorporate the structure variations of the source domain into the denoising process during training and those of target domains into the denoising during generation. These structure variations are dubbed as domain priors or domain supervisors. Nevertheless, characterizing the domain priors that can adapt to new domains is challenging because the domain priors of the target domains are not seen during training. Inspired by the impressive generalizability of masked autoencoder in both vision and language fields (He et al., 2022; Hu et al., 2022), we adopt an asymmetric encoder-decoder architecture to capture the domain priors of the source domain and to generalize to unseen structure variations from the target domains.

In what follows, we will elaborate on the design details of equivariant masked autoencoder and domain prior-supervised diffusion model in Section 3.1 and Section 3.2, respectively. Then, we will briefly summarize the training scheme and domain adaptive molecule generation in Section 3.3. The proposed GADM workflow is provided in Figure 1.

3.1. Equivariant Masked Autoencoder

Masking. For a given molecule $\mathcal{G} = \langle \mathbf{x}, \mathbf{h} \rangle$, we apply various masking strategies (\mathcal{M}) to derive the visible structure $\mathcal{G}^V = \langle \mathbf{x}^V, \mathbf{h}^V \rangle \leftarrow \mathcal{M}(\mathcal{G})$ for distinct adaptive molecule design tasks, as depicted in the right section of Figure 1. In the case of scaffold-domain and ring-domain adaptive design, we mask (*i.e.*, remove) the atoms not present on the scaffold/rings. This process is expressed as $\mathcal{G}^V \leftarrow \langle \mathbf{x} - \mathbf{x}^s, \mathbf{h} - \mathbf{h}^s \rangle$.

Variational Autoencoder. The EMAE comprises an encoder \mathcal{E} , which maps visible structure \mathcal{G}^V to a latent space, represented as $\mathbf{f}_x, \mathbf{f}_h = \mathcal{E}(\mathbf{x}^V, \mathbf{h}^V)$. Additionally, it includes a decoder \mathcal{D} that reconstructs the latent representation back to the original molecular space, denoted as $\hat{\mathbf{x}}, \hat{\mathbf{h}} = \mathcal{D}(\mathbf{f}_x, \mathbf{f}_h)$.

Our EMAE reconstructs the input by predicting the coordinates and features of each masked atom. The loss function computes the mean squared error (MSE) between the recon-

structed and original molecules in the original molecular space. The EMAE can be trained by minimizing the reconstruction objective, expressed as $\mathbf{f}(\mathcal{G}, \mathcal{D}(\mathcal{E}(\mathcal{M}(\mathcal{G}))))$. The encoder of the EMAE functions solely on the visible structure $\mathcal{M}(\mathcal{G})$, while the decoder reconstructs the input from the latent representation to the complete molecule \mathcal{G} . This asymmetric encoder-decoder design offers promising generalization (He et al., 2022) to the latent features. These features serve as domain supervisors and empower the model to generate molecules with unseen domain priors.

Equivariant MAE. However, applying general MAE in the geometric domain is non-trivial. The diffusion model within the overall framework operates in 3D molecular space and necessitates conditions to be either equivariant or invariant. Therefore, it is crucial to ensure the equivariance of the conditions extracted by EMAE. To achieve this, we design our EMAE based on the Equivariant Graph Neural Networks (EGNNs) (Satorras et al., 2021), thereby incorporating equivariance into both the encoder \mathcal{E}_ϕ and decoder \mathcal{D}_ϑ , where ϕ and ϑ are two learnable EGNNs. EMAE ensures that the latent representation \mathbf{f}_x and \mathbf{f}_h encoded by the encoder from visible structure are 3-D equivariant and k -d invariant, respectively. Consequently, EMAE extracts both invariant and equivariant conditions, as expressed below:

$$\mathbf{R}\mathbf{f}_x + \mathbf{t}, \mathbf{f}_h = \mathcal{E}_\phi(\mathbf{R}\mathbf{x}^V + \mathbf{t}, \mathbf{h}^V) \quad (4)$$

$$\mathbf{R}\hat{\mathbf{x}} + \mathbf{t}, \hat{\mathbf{h}} = \mathcal{D}_\vartheta(\mathbf{R}\mathbf{f}_x + \mathbf{t}, \mathbf{f}_h) \quad (5)$$

for all rotations \mathbf{R} and translations \mathbf{t} . Detailed architecture information about EMAE can be found in Appendix. The point-wise latent space adheres to the inherent structure of geometries \mathcal{G}^V , which facilitates learning conditions for the diffusion model and results in high-quality molecule design.

Following (Hoogeboom et al., 2022; Xu et al., 2023), to ensure that linear subspaces with the center of gravity always being zero can induce translation-invariant distributions, we define distributions of visible structures \mathbf{x}^V , latent conditions \mathbf{f}_x , and reconstructed $\hat{\mathbf{x}}$ on the subspace that $\sum_i \mathbf{x}_i^V$ (or $\mathbf{f}_{x,i}$ and $\hat{\mathbf{x}}_i$) = 0. Then the encoding and decoding processes can be formulated by $q_\phi(\mathbf{f}_x, \mathbf{f}_h | \mathbf{x}, \mathbf{h}) = \mathcal{N}(\mathcal{E}_\phi(\mathcal{M}(\mathbf{x}, \mathbf{h})), \sigma_0 \mathbf{I})$ and $p_\vartheta(\mathbf{x}, \mathbf{h} | \mathbf{f}_x, \mathbf{f}_h) = \prod_{i=1}^N p_\vartheta(x_i, h_i | \mathbf{f}_x, \mathbf{f}_h)$ and the EMAE can be optimized by:

$$\begin{aligned} \mathcal{L}_{\text{EMAE}} = & \mathbb{E}_{q_\phi(\mathbf{f}_x, \mathbf{f}_h | \mathbf{x}, \mathbf{h})} p_\vartheta(\mathbf{x}, \mathbf{h} | \mathbf{f}_x, \mathbf{f}_h) \\ & - \text{KL}[q_\phi(\mathbf{f}_x, \mathbf{f}_h | \mathbf{x}, \mathbf{h}) || \prod_i^N \mathcal{N}(f_{x,i}, f_{h,i} | 0, \mathbf{I})], \end{aligned} \quad (6)$$

where $-\mathbb{E}_{q_\phi(\mathbf{f}_x, \mathbf{f}_h | \mathbf{x}, \mathbf{h})} p_\vartheta(\mathbf{x}, \mathbf{h} | \mathbf{f}_x, \mathbf{f}_h)$ is the reconstruction loss and is calculated as L_2 norm or cross-entropy for continuous or discrete features. $\text{KL}[q_\phi(\mathbf{f}_x, \mathbf{f}_h | \mathbf{x}, \mathbf{h}) || \prod_i^N \mathcal{N}(f_{x,i}, f_{h,i} | 0, \mathbf{I})]$ is a regularization term between q_ϕ and standard Gaussians. $\mathcal{L}_{\text{EMAE}}$ is

standard VAE loss and is the variational lower bound of log-likelihood. The equivariance of the loss, which is crucial for geometric graph generation, is expressed as follows:

Theorem 3.1. \mathcal{L}_{EMAE} is an $SE(3)$ -invariant variational lower bound to the log-likelihood, i.e., for any geometries $\langle \mathbf{x}, \mathbf{h} \rangle$, we have:

$$\forall \mathbf{R} \text{ and } \mathbf{t}, \mathcal{L}_{EMAE}(\mathbf{x}, \mathbf{h}) = \mathcal{L}_{EMAE}(\mathbf{R}\mathbf{x} + \mathbf{t}, \mathbf{h}). \quad (7)$$

The theorem ensures that **EMAE** is equivariant so that the extracted condition satisfies the equivariant constraints, thereby ensuring that the conditional denoising of the geometric diffusion model is also equivariant. Detailed proof of Theorem 3.1 is given in Appendix.

In summary, **EMAE** first masks the input molecule \mathcal{G} , and then inputs the visible structure \mathcal{G}^V into the encoder \mathcal{E} to obtain equivariant latent features \mathbf{f}_x and invariant latent features \mathbf{f}_h . These features have two purposes. One is to continue to be input into the decoder \mathcal{D} for reconstruction to constrain the latent features. Secondly, it is used as the condition to supervise and control the diffusion model. The specific method of the second part will be explained in the following section.

3.2. Domain Prior-Supervised Diffusion Model

With the equivariant latent features $\langle \mathbf{f}_x, \mathbf{f}_h \rangle$, now we can utilize these features as domain supervisors for reconstructing structures \mathcal{G} while still keeping geometric properties. The latent features encoded by the mask encoder from the same molecule serve as the condition for the diffusion model. Such a similar manner to self-supervised learning enables the model to generate molecules with target structural variations, and thereby, the proposed method can perform adaptive molecule generation.

Generally, geometric diffusion models are capable of controllable generation with given conditions s by modeling conditional distributions $p(\mathbf{z}|s)$. This modeling in DMs can be implemented with conditional denoising networks $\epsilon_\theta(\mathbf{z}, t, s)$ with the critical difference that it takes additional inputs s . However, an underlying constraint of such use is the assumption that s is invariant. By contrast, a fundamental challenge for our method is that the conditions for the DM contain not only invariant features \mathbf{f}_h but also equivariant features \mathbf{f}_x . This requires the distribution $p_\theta(\mathbf{z}_{0:T})$ of our DMs to satisfy the critical invariance:

$$\forall \mathbf{R}, p_\theta(\mathbf{z}_x, \mathbf{z}_h, \mathbf{f}_x, \mathbf{f}_h) = p_\theta(\mathbf{R}\mathbf{z}_x, \mathbf{z}_h, \mathbf{R}\mathbf{f}_x, \mathbf{f}_h). \quad (8)$$

To achieve this, we should ensure that (1) the initial distribution $p(\mathbf{z}_{x,T}, \mathbf{z}_{h,T}, \mathbf{f}_x, \mathbf{f}_h)$ is invariant, which is already satisfied since $\mathbf{z}_{x,T}$ is projected down by subtracting its center of gravity after sampling from standard Gaussian noise. With

the $\mathbf{f}_x, \mathbf{f}_h$ is obtained by equivariant \mathcal{E}_ϕ (Equations 4); (2) the conditional reverse processes via θ , which is expressed as $p_\theta(\mathbf{z}_{x,t-1}, \mathbf{z}_{h,t-1}|\mathbf{z}_{x,t}, \mathbf{z}_{h,t}, \mathbf{f}_x, \mathbf{f}_h)$, are equivariant:

$$\begin{aligned} \forall \mathbf{R}, p_\theta(\mathbf{z}_{x,t-1}, \mathbf{z}_{h,t-1}|\mathbf{z}_{x,t}, \mathbf{z}_{h,t}, \mathbf{f}_x, \mathbf{f}_h) \\ = p_\theta(\mathbf{R}\mathbf{z}_{x,t-1}, \mathbf{z}_{h,t-1}, |\mathbf{R}\mathbf{z}_{x,t}, \mathbf{z}_{h,t}, \mathbf{R}\mathbf{f}_x, \mathbf{f}_h). \end{aligned} \quad (9)$$

this can be realized by implementing the denoising dynamics ϵ_θ with EGNN that satisfy the following equivariance:

$$\begin{aligned} \forall \mathbf{R} \text{ and } \mathbf{t}, \mathbf{R}\mathbf{z}_{x,t-1} + \mathbf{t}, \mathbf{z}_{h,t-1} = \\ \epsilon_\theta(\mathbf{R}\mathbf{z}_{x,t} + \mathbf{t}, \mathbf{z}_{h,t}, \mathbf{R}\mathbf{f}_x + \mathbf{t}, \mathbf{f}_h, t), \end{aligned} \quad (10)$$

In order to keep translation invariance, all the intermediate states $\mathbf{z}_{x,t}, \mathbf{z}_{h,t}$ are also required to lie on the subspace by $\sum_i \mathbf{z}_{x,t,i} = 0$ by moving the center of gravity. Analogous to Equation of diffusion model, now we can train the **DSDM** by:

$$\mathcal{L}_{DSDM} = \mathbb{E}_{\mathcal{G}, \mathcal{E}(\mathcal{M}(\mathcal{G})), \epsilon, t} [\|\epsilon - \epsilon_\theta(\mathbf{z}_{x,t}, \mathbf{z}_{h,t}, \mathbf{f}_x, \mathbf{f}_h, t)\|^2] \quad (11)$$

with $w(t)$ simply set as 1 for all steps t .

3.3. Training and Generation

Training. The training loss of the entire framework can be formulated as $\mathcal{L} = \mathcal{L}_{EMAE} + \mathcal{L}_{DSDM}$. To make the training loss tractable, we also show that \mathcal{L} is theoretically an $SE(3)$ -invariant variational lower bound of the log-likelihood and we can have:

Theorem 3.2. Let $\mathcal{L} := \mathcal{L}_{EMAE} + \mathcal{L}_{DSDM}$. With certain weights $w(t)$, \mathcal{L} is an $SE(3)$ -invariant variational lower bound to the log-likelihood.

Given the above training loss and Theorem 3.2, we can optimize **GADM** via back-propagation with reparameterizing trick (Kingma & Welling, 2013). We provide the detailed proof of Theorem 3.2 in Appendix, and a formal description of the optimization procedure in Algorithm. We follow the process of EDM (Hoogeboom et al., 2022) regarding the representation for continuous features \mathbf{x} and categorical features \mathbf{h} . For clarity, we provided the details in Appendix.

Adaptive Molecule Generation. With **GADM** trained on source dataset $\{\mathcal{G}_S\}$ and given a scaffold/ring-structure from the target domain, denoted as a \mathcal{G}_T^s , we can perform adaptive molecule generation (a scaffold adaptive generative process is illustrated in Figure 2). To sample from the model, one first inputs the \mathcal{G}_T^s into the encoder \mathcal{E}_ϕ and obtains the latent representation of \mathcal{G}_T^s denoted as $\langle \mathbf{f}_x, \mathbf{f}_h \rangle$ via reparameterization. With the latent representation of the target domain prior as condition, **DSDM** first samples $\mathbf{z}_{x,T}, \mathbf{z}_{h,T} \sim \mathcal{N}_{x,h}(\mathbf{0}, \mathbf{I})$ and then iteratively samples $\mathbf{z}_{x,t-1}, \mathbf{z}_{h,t-1} \sim p_\theta(\mathbf{z}_{x,t-1}, \mathbf{z}_{h,t-1}|\mathbf{z}_{x,t}, \mathbf{z}_{h,t}, \mathbf{f}_x, \mathbf{f}_h)$. Finally, the output molecule represented as $\langle \mathbf{x}, \mathbf{h} \rangle$ is sampled

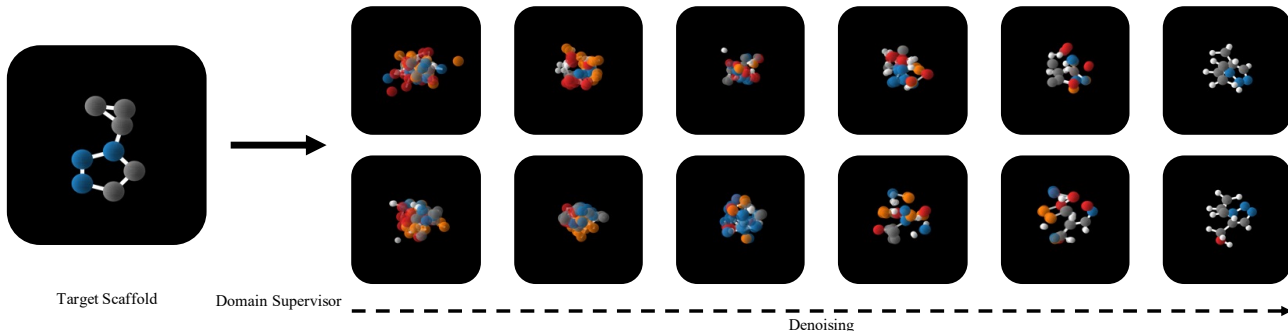


Figure 2. The illustration of the adaptive generation process with GADM: given a scaffold as the domain supervisor from a new domain, our trained GADM can generate valid, unique, and novel molecules containing the target scaffold.

from $p(\mathbf{z}_{x,0}, \mathbf{z}_{h,0} | \mathbf{z}_{x,1}, \mathbf{z}_{h,1}, \mathbf{f}_x, \mathbf{f}_h)$. The pseudo-code of the adaptive generation is provided in Algorithm in Appendix.

4. Experiments

4.1. Experiment Setup

Tasks and Datasets. We evaluate over QM9 (Ramakrishnan et al., 2014) and the GEOM-DRUG (Axelrod & Gómez-Bombarelli, 2022). Specifically, QM9 is a standard dataset that contains molecular properties and atom coordinates for 130k 3D molecules with up to 9 heavy atoms and up to 29 atoms, including hydrogens. GEOM-DRUG encompasses around 450,000 molecules, each with an average of 44.2 atoms and a maximum of 181.

Ring-Structure-Domain Adaptive Molecule Generation. In this task, ring-structure variations result in distribution shifts. We used RDKit (Landrum et al., 2016) to categorize molecules into 9 groups based on the number of rings, ranging from 0 to 8. As the number of rings increases, the quantity of molecules correspondingly decreases. We partition the QM9 dataset into two subsets based on ring count. The source domain comprises molecules and those with 0 to 3 rings, and we consider the target domains including molecules with 4 to 8 rings, respectively. Figure in the Appendix presents a schematic diagram illustrating example molecules with 0 to 8 rings. The GEOM-DRUG dataset contains molecules with 0 to 14 rings and 22 rings. We use the subsets with 0 to 10 rings as the source domain and consider five target domains, including 11 to 14 and 22. This is because the number of molecules possessing 11 to 14 and 22 rings are all under 100, representing a micro fraction of the total molecule count.

Scaffold-Domain Adaptive Molecule Generation. In this task, scaffold variations incur distribution shifts. Similarly, we utilized RDKit (Landrum et al., 2016) to examine the scaffold of each molecule within the QM9 dataset¹. Molecules

¹<https://springernature.figshare.com/ndownloader/files/3195389>

lacking a scaffold were denoted as ‘-’ and were included in the total scaffold count. The entire dataset was divided based on scaffold frequency. Specifically, the source domain contained 100,000 molecules and 1,054 scaffolds — most scaffolds appeared at least 100 times. The target domain I included 15,000 molecules and 2,532 scaffolds, where most scaffold’s frequency is between 10 to 100. The target domain II consisted of 15,831 molecules and 12,075 scaffolds; each scaffold’s frequency is less than 10. We aim to learn a generative model with the source domain training data, which can adaptively generate effective molecules that fall into desired new domains, such as target domain I/II.

Baselines. Our work is the first to consider the problem of domain adaptive generation for 3D molecules, leading to the absence of baselines for a comprehensive comparison. As alternatives, we employ three state-of-the-art 3D molecule diffusion models, EDM (Hoogeboom et al., 2022), GeoLDM (Xu et al., 2023) and EEGSDE (Bao et al., 2023), as baselines to validate the efficacy of our proposed GADM. These methods can perform controllable generation but can only control the generation process with numerical features. Intuitively, the number of rings could be a numerical feature of a molecule. We treat the ring counts as one control factor to manipulate the generation process of the baselines, denoted as C-EDM, C-GeoLDM, and EEGSDE to verify GADM’s effectiveness in the ring-structure domain adaptive generation task (see Table 2).

Metrics. The objective of the adaptive generation problem is to generate effective 3D molecules in a target new domain. A generated sample is effective only when it falls into the target domain while it is valid, unique, and novel simultaneously. Therefore, our evaluation metrics can be defined as follows:

1. **Proportion (P):** Given a target scaffold/ring set $\{\mathcal{G}_T^s\}$, proportion describes the percentage of molecules that contain the desired scaffold/ring-structure in $\{\mathcal{G}_T^s\}$ among generated valid samples;
2. **Coverage (C):** Coverage describes the percentage of scaffolds set of the generated samples (denoted as $\{\mathcal{G}_G^s\}$) in target scaffolds set $\{\mathcal{G}_T^s\}$, which is expressed as $C = |\{\mathcal{G}_G^s\} \cap \{\mathcal{G}_T^s\}| / |\{\mathcal{G}_T^s\}|$;
3. **Target validity (V):** The percentage

Table 2. Results of molecule proportion in terms of ring-number (P), molecule validity (V), novelty (N), and success rate (S). The best results are highlighted in bold. QM9 only contains 36 eight-ring molecules, and the proportion for eight-ring is nearly 0.

Metrics Domains	P (%) in Source Domain				P (%) in Target Domains					AS (%)	MS (%)	V (%)	N (%)	S (%)
	0	1	2	3	4	5	6	7	8					
QM9	10.2	39.3	27.6	15.1	4.4	2.7	0.6	0.2	0.0	99.0	95.2	97.7	-	-
EDM†	10.5	39.8	28.0	14.5	4.0	2.9	0.2	0.1	0.0	11.0	9.6	10.4	6.8	6.3
GeoLDM†	12.0	38.6	27.0	15.3	4.6	2.2	0.2	0.1	0.0	11.0	9.9	10.4	6.4	5.9
EDM‡	12.1	44.1	29.8	11.8	1.7	0.5	0.0	0.0	0.0	11.0	9.7	10.4	6.8	6.3
GeoLDM‡	2.8	41.5	32.1	15.7	4.7	2.7	0.3	0.1	0.0	10.9	9.1	10.4	6.7	6.2
C-EDM‡	98.9	94.2	80.8	64.4	12.6	26.8	0.3	0.1	0.0	41.3	33.9	38.0	27.3	24.1
C-GeoLDM‡	97.1	89.4	74.2	52.4	22.3	22.7	0.9	0.2	0.0	39.1	31.5	35.7	28.3	25.0
EEGSDE‡	98.4	92.2	77.6	58.2	14.1	17.6	0.3	0.0	0.0	39.1	31.1	35.7	27.2	24.2
GADM‡	99.9	99.8	99.1	97.6	92.5	89.7	78.7	88.2	82.1	83.1	54.0	77.9	70.3	40.5

†: Models are trained over entire QM9; ‡: Models are trained over ring-split QM9 with ring-number from 0-3.

C-: C-EDM and C-GeoLDM are trained with conditioning on ring counts.

Table 3. Results of molecule proportion in terms of ring-number (P), atom stability (AS), molecule validity (V), novelty (N), and success rate (S). The number of molecules with above 11 rings in GEOM-DRUG is lower than 100.

Averaged metrics (%) over 5 Ring Domains (11, 12, 13, 14, and 22)					
Method	P (%)	AS (%)	V (%)	N (%)	S (%)
GEOM-DRUG	0.0	86.5	99.9	-	-
EDM†	0.0	0.0	0.0	0.0	0.0
GeoLDM†	0.0	0.0	0.0	0.0	0.0
GADM‡	13.8	11.4	11.0	13.8	10.9

‡ Models are trained on GEOM-DRUG with ring number from 0-10.

of valid molecules among all the desired molecules, which is measured by RDKit (Landrum et al., 2016) and widely used for calculating validity (Hoogeboom et al., 2022; Xu et al., 2023)); 4. **Target novelty (N)**: The percentage of novel molecules among all the desired valid molecules, the novel molecule is different from training samples; 5. **Success rate (S)**: The ratio of generated valid, unique, and novel molecules that contain the desired scaffold/ring-structure. 6. **Target atom stability (AS)**: The ratio of atoms that has the correct valency among the molecules with the desired scaffold/ring-structure. 7. **Target molecule stability (MS)**: The ratio of generated molecules contains the desired scaffold/ring-structure, and all atoms are stable.

4.2. Results and Analysis

Ring-Structure Domain Adaptive Molecule Generation.

In this task, all models were trained with the same source domain that contains molecules with ring counts ranging from 0 to 3, and subsequently, their performances were tested for generating molecules with 4 to 8 rings, respectively. We present the results on 10,000 generated molecules for each ring-count domain in Table 2. For clarity, the generated target molecule validity, novelty, and success rate are calculated by averaging the corresponding values from the source domain and 5 target domains, and more comprehensive results are presented in Appendix.

Table 2 demonstrates that those uncontrollable version of baselines (i.e., EDM and GeoLDM) can barely generate molecules with 4 to 8 rings — 4.6% at most. Manipulating the generation process with ring counts can slightly improve out-of-domain generation performance with up to 25% success rates. In contrast, **GADM** can achieve a 40.5% success rate. Moreover, we observe that no baselines can generate 8-ring molecules, including those controllable generation methods (i.e., C-GeoLDM, C-EDM, and EEGSDE), reflecting the difficulty of generating those complex molecules rare existing in the original QM9 (only 36 8-ring molecules). Notably, **GADM** can generate 82.1% portion of 8-ring domain molecules even though the training data does not contain any of those samples, showing the significance of using structural-grained representations for controlling the denoising process of the diffusion models. Specifically, among the generated 10,000 molecules using **GADM**, 2,388 valid, unique, and novel 8-ring molecules exist. These results verify that **GADM** can adaptively generate 3D molecules from the desired new domains regarding ring-structure variations.

Table 3 presented the statistical results of various methods for generating rare ring number molecules (ranging from 11 to 14 and 22) on the large-scale dataset GEOM-DRUG. Notably, EDM and GeoLDM, which are trained on the complete dataset, are incapable of generating molecules with ring numbers exceeding 10, thus failing to produce any desired molecules. In contrast, **GADM** can generate an average of 13.8% of the desired molecules. Particularly, for molecules with 22 rings, of which there are only two in the original dataset, **GADM** achieves a remarkable success rate of 13.7% in generating such molecules, even without training on these two molecules.

Scaffold-Domain Adaptive Molecule Generation. In the task of scaffold-domain adaptive molecule generation, the baselines are trained on both the entire dataset (†) and solely on the source domain (‡), respectively. In contrast, our **GADM** is trained exclusively over the source domain dataset. After training, each model generates 15,000

Table 4. Results of proportion (P), scaffold coverage (C), molecule validity (V), molecule novelty (N), and molecule success rate (S). The best results are highlighted in bold.

Domains	Source Domain (%)					Target Domain I (%)					Target Domain II (%)				
# Metric	P	C	V	N	S	P	C	V	N	S	P	C	V	N	S
Data	76.4	100.0	97.7	-	-	11.5	100.0	97.7	-	-	12.1	100.0	97.7	-	-
EDM†	79.9	36.3	74.8	48.8	45.0	10.9	28.9	10.2	6.7	6.1	9.2	34.9	8.6	5.6	5.2
GeoLDM†	80.4	35.2	75.6	46.7	43.1	10.7	31.2	10.1	6.2	5.8	8.8	33.5	8.3	5.1	4.7
EDM‡	91.4	56.5	83.2	58.2	52.0	5.9	26.5	5.3	3.7	3.3	2.7	17.0	2.4	1.7	1.5
GeoLDM‡	90.6	54.3	81.7	57.8	51.0	5.9	26.7	5.3	3.8	3.3	3.5	19.0	3.2	2.3	2.0
GADM‡	99.2	92.5	90.7	67.6	52.4	97.0	97.1	80.0	84.5	68.9	95.5	85.7	83.3	82.0	65.8

† Models are trained over the entire QM9 dataset.

‡ Models are trained only on the source domain, where each scaffold appears at least 100 times.

Table 5. Results of atom stability (AS) and molecule stability (MS). The best results are highlighted in bold.

Domains	Source Domain		Target Domain I		Target Domain II	
# Metric (%)	AS	MS	AS	MS	AS	MS
Data	75.7	72.8	11.4	10.9	12.0	11.5
EDM†	78.9	65.5	9.1	7.5	10.8	8.9
GeoLDM†	79.5	71.9	8.7	7.9	10.6	9.6
EDM‡	90.4	73.3	2.6	2.1	5.8	4.7
GeoLDM‡	89.1	75.6	3.5	3.0	5.8	4.9
GADM‡	96.1	71.3	89.0	35.1	89.5	45.6

molecules for the source domain and target domains I and II, respectively. The quantitative results using various metrics are presented in Table 4, Table 5 and Figure 3. We observe that with EDM or GeoLDM, the scaffold proportion of the generated molecules indeed mirrors that of the training samples (see proportion and coverage visualization in Figure 3). However, they all struggle to generate molecules with scaffolds falling into targeted domain I or II; they can only achieve 3.3% success rates at most (see EDM‡ and GeoLDM‡ in Table 4). In contrast, our proposed GADM, trained solely on the source domain, can generate molecules containing the target scaffolds under the corresponding supervision, achieving at least 95.5% proportion in both new domains. Note that the target scaffolds were not seen during training.

Moreover, we found that GADM can reach 92.5% coverage for the in-domain generation with the in-domain supervisor — structural-grained representations from the latent space of EMAE. Notably, even for target domain II, comprising over 12k different rare scaffolds, GADM can achieve 85.7% coverage. Nevertheless, all baselines can only achieve 56.6% coverage at most, indicating the significance of our EMAE. It is worth noting that GADM does not need any target molecules but uses the scaffold as the domain supervisor for cross-domain adaptation, bypassing the obstacles due to data scarcity. GADM improves the molecule novelty and success rate by up to 80.8% regarding novelty and 65.6% in terms of success rate as compared to the baselines. The atom stability and molecule stability presented in Table 5

also demonstrates that the designed GADM performs better on generating chemically stable molecules with desired scaffolds.

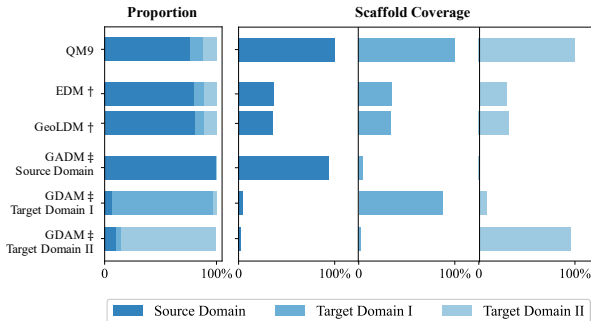


Figure 3. Scaffolds Proportion and Coverage.

Discussion. Our experiments reveal that existing generative models may generate a limited number of molecules with unseen scaffolds or ring-structures, as shown in Tables 2 and 4. This phenomenon may be attributed to the fact that scaffolds/ring-structures in different domains may be mutually inclusive or share substructures. Consequently, the generated molecules may contain sub-structures or mixed structures derived from the training samples, thereby constituting unseen scaffolds/ring-structures. However, such out-of-domain generation is relatively trivial and less controllable compared to the proposed method since the empirical studies presented above underscore the significant potential of the proposed GADM in generating molecules with targeted structural variations, including scaffold and ring-structure domains.

5. Related Work

Molecule Generation Models. Prior studies on molecule generation focused on generating molecules as 2D graphs (Jin et al., 2018; Liu et al., 2018; Shi et al., 2020). However, there has been a growing interest in 3D molecule generation. G-SchNet (Gebauer et al., 2019) and G-SphereNet (Luo & Ji, 2022) utilize autoregressive techniques to construct molecules incrementally by progres-

sively connecting atoms or molecular fragments. These frameworks necessitate either a meticulous formulation of complex action space or action ordering.

More recently, the focus has shifted towards using Diffusion Models (DMs) for 3D molecule generation (Hoogeboom et al., 2022; Xu et al., 2023; Wu et al., 2022; Song et al., 2024b). To mitigate the inconsistency of unified Gaussian diffusion across diverse modalities, a latent space was introduced by (Xu et al., 2023). To tackle the atom-bond inconsistency problem, different noise schedulers were proposed by (Peng et al., 2023) for various modalities to accommodate noise sensitivity. However, these algorithms do not account for generating novel molecules outside the training domain.

Domain Adaptive Generation. Domain adaptive generation, although under-explored, is of paramount importance, especially considering that molecules generated by machine-learning methods often exhibit a “striking similarity” (Walters & Murcko, 2020). In recent years, some preliminary work has begun to use reinforcement learning (Yang et al., 2021) and out-of-distribution control (Lee et al., 2023) to explore the generation of novel molecules. However, these methods are still challenging when designing novel molecules for the target domain. As proposed by (Lee et al., 2023), MOOD employs an OOD control and integrates a conditional score-based diffusion scheme to optimize molecules for specific chemical properties. Similarly, MuDM uses property prediction models to address single and multiple property objectives in molecule generation (Han et al., 2024). However, these methods fail to generate novel molecules with target properties that have yet to be learned by either the generative or additional prediction models.

6. Conclusion

This paper introduced the problem of domain adaptive molecule generation, which entails assessing the ability of a trained diffusion-based generator to produce 3D molecules for a new domain. To address this problem, the proposed GADM captures the structural-grained representations of the in-domain samples using a masked VAE and various masking strategies. The structural-grained representations then act as domain supervisors to control the denoising process. Thorough experimental studies have demonstrated that the trained model can adaptively generate target, valid, unique, and novel molecules, enhancing the success rate by up to 60%. Our work responds positively to the question posed at the beginning of the abstract and paves the way for practical artificial intelligence-aid molecule discovery.

Impact Statements

This paper presents work whose goal is to advance the field of generative Artificial Intelligence (AI) for scientific fields, such as material science, chemistry, and biology. The obtained experience/knowledge will greatly boost generative AI technologies in facilitating the process of scientific knowledge discovery.

References

- Axelrod, S. and Gómez-Bombarelli, R. Geom, energy-annotated molecular conformations for property prediction and molecular generation. *Scientific Data*, 9(1):185, 2022. ISSN 2052-4463. doi: 10.1038/s41597-022-01288-4.
- Bao, F., Zhao, M., Hao, Z., Li, P., Li, C., and Zhu, J. Equivariant energy-guided SDE for inverse molecular design. In *The Eleventh International Conference on Learning Representations*, 2023.
- Bemis, G. W. and Murcko, M. A. The properties of known drugs. 1. molecular frameworks. *Journal of Medicinal Chemistry*, 39(15):2887–2893, 1996.
- Celeghini, E., Giachetti, R., Sorace, E., and Tarlini, M. The three-dimensional euclidean quantum group $e(3)_q$ and its r -matrix. *Journal of Mathematical Physics*, 32(5):1159–1165, 1991.
- Garcia Satorras, V., Hoogeboom, E., Fuchs, F., Posner, I., and Welling, M. E(n) equivariant normalizing flows. In Ranzato, M., Beygelzimer, A., Dauphin, Y., Liang, P., and Vaughan, J. W. (eds.), *Advances in Neural Information Processing Systems*, volume 34, pp. 4181–4192. Curran Associates, Inc., 2021.
- Gebauer, N., Gastegger, M., and Schütt, K. Symmetry-adapted generation of 3d point sets for the targeted discovery of molecules. In Wallach, H., Larochelle, H., Beygelzimer, A., d’Alché-Buc, F., Fox, E., and Garnett, R. (eds.), *Advances in Neural Information Processing Systems*, volume 32. Curran Associates, Inc., 2019.
- Han, X., Shan, C., Shen, Y., Xu, C., Yang, H., Li, X., and Li, D. Training-free multi-objective diffusion model for 3d molecule generation. In *The Twelfth International Conference on Learning Representations*, 2024.
- He, K., Chen, X., Xie, S., Li, Y., Dollár, P., and Girshick, R. Masked autoencoders are scalable vision learners. In *Proceedings of the IEEE/CVF Conference on Computer Vision and Pattern Recognition (CVPR)*, pp. 16000–16009, June 2022.
- Ho, J., Jain, A., and Abbeel, P. Denoising diffusion probabilistic models. In Larochelle, H., Ranzato, M., Hadsell,

- R., Balcan, M., and Lin, H. (eds.), *Advances in Neural Information Processing Systems*, volume 33, pp. 6840–6851. Curran Associates, Inc., 2020.
- Hoogeboom, E., Satorras, V. G., Vignac, C., and Welling, M. Equivariant diffusion for molecule generation in 3D. In Chaudhuri, K., Jegelka, S., Song, L., Szepesvari, C., Niu, G., and Sabato, S. (eds.), *Proceedings of the 39th International Conference on Machine Learning*, volume 162 of *Proceedings of Machine Learning Research*, pp. 8867–8887. PMLR, 17–23 Jul 2022.
- Hu, D., Hou, X., Du, X., Zhou, M., Jiang, L., Mo, Y., and Shi, X. VarMAE: Pre-training of variational masked autoencoder for domain-adaptive language understanding. In Goldberg, Y., Kozareva, Z., and Zhang, Y. (eds.), *Findings of the Association for Computational Linguistics: EMNLP 2022*, pp. 6276–6286, Abu Dhabi, United Arab Emirates, December 2022. Association for Computational Linguistics. doi: 10.18653/v1/2022.findings-emnlp.468.
- Jin, W., Barzilay, R., and Jaakkola, T. Junction tree variational autoencoder for molecular graph generation. In Dy, J. and Krause, A. (eds.), *Proceedings of the 35th International Conference on Machine Learning*, volume 80 of *Proceedings of Machine Learning Research*, pp. 2323–2332. PMLR, 10–15 Jul 2018.
- Karageorgis, G., Warriner, S., and Nelson, A. Efficient discovery of bioactive scaffolds by activity-directed synthesis. *Nature Chemistry*, 6(10):872–876, 2014. ISSN 1755-4349. doi: 10.1038/nchem.2034.
- Kingma, D. P. and Welling, M. Auto-encoding variational bayes. In *2nd International Conference on Learning Representations*, 2013.
- Landrum, G. et al. Rdkit: Open-source cheminformatics software. 2016.
- Lee, S., Jo, J., and Hwang, S. J. Exploring chemical space with score-based out-of-distribution generation. In Krause, A., Brunskill, E., Cho, K., Engelhardt, B., Sabato, S., and Scarlett, J. (eds.), *Proceedings of the 40th International Conference on Machine Learning*, volume 202 of *Proceedings of Machine Learning Research*, pp. 18872–18892. PMLR, 23–29 Jul 2023.
- Liu, Q., Allamanis, M., Brockschmidt, M., and Gaunt, A. Constrained graph variational autoencoders for molecule design. In Bengio, S., Wallach, H., Larochelle, H., Grauman, K., Cesa-Bianchi, N., and Garnett, R. (eds.), *Advances in Neural Information Processing Systems*, volume 31. Curran Associates, Inc., 2018.
- Luo, Y. and Ji, S. An autoregressive flow model for 3d molecular geometry generation from scratch. In *International Conference on Learning Representations*, 2022.
- Peng, X., Guan, J., Liu, Q., and Ma, J. Moldiff: Addressing the atom-bond inconsistency problem in 3d molecule diffusion generation. *arXiv preprint arXiv:2305.07508*, 2023.
- Qian, K. and Yu, Z. Domain Adaptive Dialog Generation via Meta Learning. In *Proceedings of the 57th Annual Meeting of the Association for Computational Linguistics*, pp. 2639–2649, 2019.
- Ramakrishnan, R., Dral, P. O., Rupp, M., and von Lilienfeld, O. A. Quantum chemistry structures and properties of 134 kilo molecules. *Scientific Data*, 1(1):140022, 2014. ISSN 2052-4463.
- Ritchie, T. J. and Macdonald, S. J. The impact of aromatic ring count on compound developability – are too many aromatic rings a liability in drug design? *Drug Discovery Today*, 14(21):1011–1020, 2009. ISSN 1359-6446.
- Satorras, V. G., Hoogeboom, E., and Welling, M. E(n) equivariant graph neural networks. In Meila, M. and Zhang, T. (eds.), *Proceedings of the 38th International Conference on Machine Learning*, volume 139 of *Proceedings of Machine Learning Research*, pp. 9323–9332. PMLR, 18–24 Jul 2021.
- Serre, J.-P. et al. *Linear representations of finite groups*, volume 42. Springer, 1977.
- Shi, C., Xu, M., Zhu, Z., Zhang, W., Zhang, M., and Tang, J. Graphaf: a flow-based autoregressive model for molecular graph generation. In *International Conference on Learning Representations*, 2020.
- Sohl-Dickstein, J., Weiss, E., Maheswaranathan, N., and Ganguli, S. Deep unsupervised learning using nonequilibrium thermodynamics. In Bach, F. and Blei, D. (eds.), *Proceedings of the 32nd International Conference on Machine Learning*, volume 37 of *Proceedings of Machine Learning Research*, pp. 2256–2265, Lille, France, 07–09 Jul 2015. PMLR.
- Song, K., Han, L., Liu, B., Metaxas, D., and Elgammal, A. StyleGAN-Fusion: Diffusion Guided Domain Adaptation of Image Generators. In *Proceedings of the IEEE/CVF Winter Conference on Applications of Computer Vision*, pp. 5453–5463, 2024a.
- Song, Y., Gong, J., Qu, Y., Zheng, M., Zhou, H., Liu, J., and Ma, W.-Y. Unified generative modeling of 3d molecules with bayesian flow networks. In *The Twelfth International Conference on Learning Representations*, 2024b.

- Walters, W. P. and Murcko, M. Assessing the impact of generative ai on medicinal chemistry. *Nature Biotechnology*, 38(2):143–145, 2020. ISSN 1546-1696.
- Ward, S. E. and Beswick, P. What does the aromatic ring number mean for drug design? *Expert Opinion on Drug Discovery*, 9(9):995–1003, 2014. doi: 10.1517/17460441.2014.932346. PMID: 24955724.
- Watson, J. L., Juergens, D., Bennett, N. R., Trippe, B. L., Yim, J., Eisenach, H. E., Ahern, W., Borst, A. J., Ragotte, R. J., Milles, L. F., Wicky, B. I. M., Hanikel, N., Pellock, S. J., Courbet, A., Sheffler, W., Wang, J., Venkatesh, P., Sappington, I., Torres, S. V., Lauko, A., De Bortoli, V., Mathieu, E., Ovchinnikov, S., Barzilay, R., Jaakkola, T. S., DiMaio, F., Baek, M., and Baker, D. De novo design of protein structure and function with rfdiffusion. *Nature*, 620(7976):1089–1100, 2023. ISSN 1476-4687.
- Wu, L., Gong, C., Liu, X., Ye, M., and qiang liu. Diffusion-based molecule generation with informative prior bridges. In Oh, A. H., Agarwal, A., Belgrave, D., and Cho, K. (eds.), *Advances in Neural Information Processing Systems*, 2022.
- Wu, Z., Ramsundar, B., Feinberg, E. N., Gomes, J., Geniesse, C., Pappu, A. S., Leswing, K., and Pande, V. Moleculenet: a benchmark for molecular machine learning. *Chem Sci*, 9(2):513–530, 2018. ISSN 2041-6520 (Print) 2041-6520. doi: 10.1039/c7sc02664a.
- Xie, T., Fu, X., Ganea, O.-E., Barzilay, R., and Jaakkola, T. S. Crystal diffusion variational autoencoder for periodic material generation. In *International Conference on Learning Representations*, 2022.
- Xu, M., Powers, A. S., Dror, R. O., Ermon, S., and Leskovec, J. Geometric latent diffusion models for 3D molecule generation. In Krause, A., Brunskill, E., Cho, K., Engelhardt, B., Sabato, S., and Scarlett, J. (eds.), *Proceedings of the 40th International Conference on Machine Learning*, volume 202 of *Proceedings of Machine Learning Research*, pp. 38592–38610. PMLR, 23–29 Jul 2023.
- Yang, S., Hwang, D., Lee, S., Ryu, S., and Hwang, S. J. Hit and lead discovery with explorative rl and fragment-based molecule generation. In Ranzato, M., Beygelzimer, A., Dauphin, Y., Liang, P., and Vaughan, J. W. (eds.), *Advances in Neural Information Processing Systems*, volume 34, pp. 7924–7936. Curran Associates, Inc., 2021.
- Yang, Z., Hu, J., Salakhutdinov, R., and Cohen, W. Semi-Supervised QA with Generative Domain-Adaptive Nets. In *Proceedings of the 55th Annual Meeting of the Association for Computational Linguistics (Volume 1: Long Papers)*, pp. 1040–1050, 2017.